Appendix 3

Dynamic restitution of action potential duration during electrical alternans and ventricular fibrillation

MARCUS L. KOLLER, MARK L. RICCIO, AND ROBERT F. GILMOUR, JR.
Department of Physiology, Cornell University, Ithaca, New York 14853-6401

Koller, Marcus L., Mark L. Riccio, and Robert F. Gilmour, Jr. Dynamic restitution of action potential duration during electrical alternans and ventricular fibrillation. *Am. J. Physiol.* 275 (*Heart Circ. Physiol.* 44): H1635–H1642, 1998.—The restitution kinetics of action potential duration (APD) were investigated in paced canine Purkinje fibers (P; $n = 9$) and endocardial muscle (M; $n = 9$), in isolated, perfused canine left ventricles during ventricular fibrillation (VF; $n = 4$), and in endocardial muscle paced at VF cycle lengths (simulated VF; $n = 4$). Restitution was assessed with the use of two protocols: delivery of a single extrastimulus after a train of stimuli at cycle length = 300 ms (standard protocol), and fixed pacing at short cycle lengths (100–300 ms) that induced APD alternans (dynamic protocol). The dynamic protocol yielded a monotone increasing restitution function with a maximal slope of 1.13 ± 0.13 in M and 1.14 ± 0.17 in P. Iteration of this function reproduced the APD dynamics found experimentally, including persistent APD alternans. In contrast, the standard protocol yielded a restitution relation with a maximal slope of 0.57 ± 0.18 in M and 0.84 ± 0.20 in P, and iteration of this function did not reproduce the APD dynamics. During VF, the restitution kinetics at short diastolic interval were similar to those determined with the dynamic protocol (maximal slope: 1.72 ± 0.47 in VF and 1.44 ± 0.49 in simulated VF). Thus APD dynamics at short coupling intervals during fixed pacing and during VF were accounted for by the dynamic, but not the standard, restitution relation. These results provide further evidence for a strong relationship among the kinetics of electrical restitution, the occurrence of APD alternans, and complex APD dynamics during VF.

restitution kinetics; complex dynamics; ventricular arrhythmias

RATE-DEPENDENT ALTERATIONS of action potential duration (APD) and refractoriness are believed to be important determinants of ventricular arrhythmias (6, 7, 9, 13, 16, 17, 19, 23, 28, 30). The changes in APD that accompany changes in rate reflect the dependence of APD on the preceding diastolic interval (DI), a relationship characterized by electrical restitution (2–4, 10–12). Several experimental and computer modeling studies (9, 15–17, 19, 20, 26) have suggested that the kinetics of electrical restitution have important implications for the development of ventricular arrhythmias. In particular, it has been proposed that a steep slope (≥ 1) of the restitution relation may determine whether single spiral waves of electrical activity splinter into multiple smaller spirals, thereby creating a transition from ventricular tachycardia to ventricular fibrillation (5, 17, 31).

The breakup of spiral waves is thought to be precipitated by oscillations of APD that are of sufficiently large amplitude to cause conduction block along the spiral wave front (17). This type of oscillation, also known as APD alternans, is a well-recognized phenomenon that occurs in ventricular tissue at rapid rates of stimulation and after abrupt shortening of the cycle length (21, 25, 26). During alternans, a short (long) DI sequence generates a short (long) APD sequence. This dynamic property is linked to the slope of the restitution relation in that, for persistent APD alternans to occur, the restitution relation must have a region of slope ≥ 1 (6, 13, 14, 21, 30). However, in most studies the slope of the restitution relation, when determined with a standard protocol (3, 4, 10–12), has been reported to be <1 (13, 16, 19, 25–27). One possible explanation for this discrepancy is that changes in restitution kinetics secondary to rapid accumulation and dissipation of memory may not be accounted for by the standard restitution relation (13).

If the standard restitution relation cannot account for APD dynamics during rapid pacing, might it also not account for APD dynamics during ventricular tachyarrhythmias, such as ventricular fibrillation? Conversely, if the restitution relation during APD alternans could be determined directly, might such a relation more closely approximate the restitution relation during ventricular fibrillation?

To address these questions, we determined the relationship between APD and DI during rapid pacing at cycle lengths that produced APD alternans (dynamic restitution relation) and compared that relationship with the relationship between APD and DI obtained using a standard S1-S2 protocol (standard restitution relation). We then determined whether dynamic or standard restitution more closely approximated the restitution relation that pertains during ventricular fibrillation. Our results indicate that dynamic restitution accounts for the restitution relation during rapid pacing and during ventricular fibrillation. Accordingly, dynamic restitution should be considered during assessment of interventions that may facilitate or inhibit the development of ventricular tachyarrhythmias.

MATERIALS AND METHODS

Adult mongrel dogs of either sex weighing 10–30 kg were anesthetized with Fatal-Plus (390 mg/ml pentobarbital sodium; 86 mg/kg iv; Vortech Pharmaceuticals, Dearborn, MI), and their hearts were excised rapidly and placed in cool Tyrode solution. Thin (~2 mm thick) sheets of endocardium ($n = 9$) measuring 2 × 1 cm and free running Purkinje fibers ($n = 9$) that were 10–20 mm in length and 2–4 mm in width

The costs of publication of this article were defrayed in part by the payment of page charges. The article must therefore be hereby marked "*advertisement*" in accordance with 18 U.S.C. Section 1734 solely to indicate this fact.

were excised from either ventricle using fine scissors. The tissues were mounted in a Plexiglas chamber and were superfused with normal Tyrode solution at a rate of 15 ml/min. The Tyrode solution was bubbled with 95% O_2-5% CO_2. The Po_2 was 400–600 mmHg, the pH was 7.35 ± 0.05, and the temperature was 37.0 ± 0.5°C. The composition of the Tyrode solution (in mM) was 0.5 $MgCl_2$, 0.9 NaH_2PO_4, 2.0 $CaCl_2$, 137.0 NaCl, 24.0 $NaHCO_3$, 4.0 KCl, and 5.5 glucose.

Initially, the fibers were stimulated during a recovery period of at least 60 min at a basic cycle length (BCL) of 500 ms. Rectangular pulses of 2-ms duration and two to three times the diastolic threshold (0.1–0.3 mA) were delivered through Teflon-coated bipolar silver electrodes using a computer-controlled stimulator. Transmembrane action potentials were recorded with machine-pulled glass capillary electrodes filled with 3 M KCl. Recordings were obtained from sites located within 1–3 mm of the bipolar stimulating electrode. Typically, the site of impalement was midway between the poles of the stimulating electrode (which were 1 mm apart) to minimize the stimulus artifact and the effects of current polarity.

Standard restitution protocol. The dependence of APD on the preceding DI was determined with the use of a standard S1-S2 protocol, as described by us (13, 28) and by others (3, 4, 10–12, 17) previously. Single test pulses (S2) were delivered after every 20th basic pulse (S1) at a BCL of 300 ms (see Fig. 1*A*). This BCL was used because it was the shortest cycle length at which no alternation of APD occurred in any of the fibers. The S1-S2 coupling interval was progressively shortened in steps of 10–20 ms starting from 300 ms until the premature pulse was blocked. The S1-S2 interval was then increased by 20 ms to restore capture and was subsequently shortened in 1–2 ms decrements until S2 was blocked. The duration of the response to S2 was measured from the stimulus artifact to 95% of repolarization (APD_{95}) with a precision of 1 ms and was plotted as a function of the preceding DI, where the DI equaled the S1-S2 interval minus APD_{95} of the response to the last S1 stimulus.

The time course of restitution was fit using a sigmoid function of the type $APD = a + b/[1 + \exp[-(DI - c)/d]]$. The sigmoid function fit the experimental data with r^2 coefficients >0.98 in every experiment and was superior to previously described mono- and biexponential fits (10, 11, 26). The sigmoid function fit the data better than mono- or biexponential fits because APD at very short (i.e., negative) DI was prolonged, secondary to increased latency, as described previously (6, 7, 13). Because the microelectrode was very close to the stimulating electrode, the latency between delivery of the stimulus and the onset of the action potential was never greater than the duration of the stimulus (2 ms). However, at short DI, a latency occurred between the onset of the action potential and the peak voltage attained during phase zero. This latency was manifest as an apparently electrotonic deflection preceding a more rapid upstroke or simply as a slow upstroke. In either case, the latency contributed to the duration of the cellular response and for that reason was included in the measurement of APD.

Dynamic restitution protocol. For the dynamic protocol, the fibers initially were paced at a constant BCL of 400 ms. After 50 stimuli had been delivered at this BCL, pacing was stopped and APD_{95} of the last paced action potential was measured. Pacing was then reinitiated at a shorter BCL, and APD_{95} was determined after 50 stimuli had been delivered at the new BCL. The BCL was shortened in steps of 50 ms for BCL >200 ms and in steps of 5–10 ms for BCL <200 ms. At BCL <250 ms, APD alternans occurred. During APD alternans, pacing was interrupted twice to directly measure APD_{95} of both the long and the short action potential (Fig. 1*B*). The BCL was shortened until either 2:1 block or higher-order periodicities (e.g., 4:4 stimulus-response locking) occurred.

For these experiments, action potential data were acquired and analyzed in real time. The take-off potential (TOP), defined as the membrane voltage at the moment of the delivery of the stimulus, was monitored continuously. At cycle lengths that produced APD alternans, a minimum of 50 stimuli were delivered at a given BCL and pacing was then

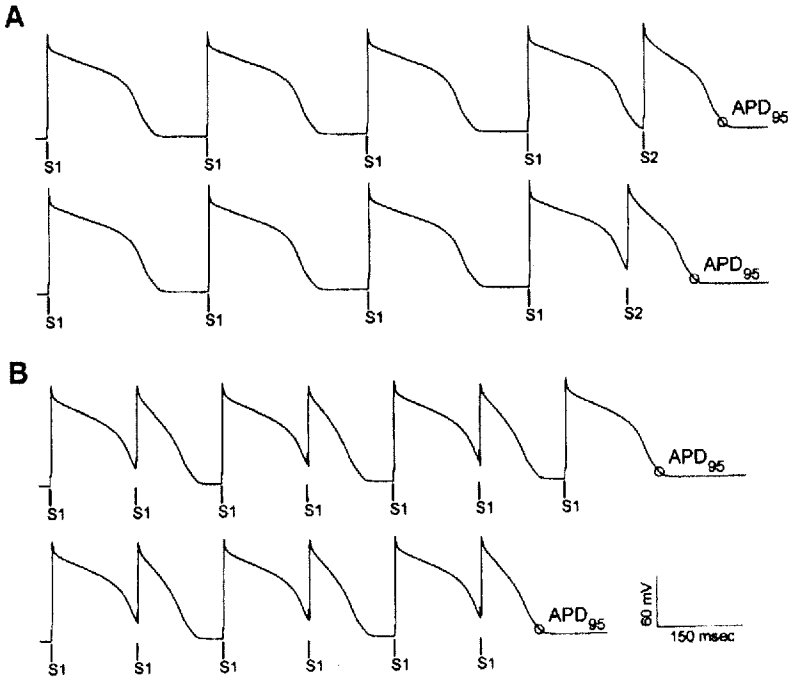

Fig. 1. *A*: standard restitution protocol. The fiber is paced at a constant S1-S1 interval followed by a single premature stimulus (S2) at progressively shorter S1-S2 intervals. Action potential duration at 95% of repolarization (APD_{95}) of the response to S2 is measured. S1, basic pulse. *B*: dynamic restitution protocol. The fiber is paced at progressively shorter S1-S1 intervals until APD alternans occurs. During alternans, pacing is interrupted once after the long action potential (*top tracing*) and once after the short action potential (*bottom tracing*), which allows for direct measurement of APD_{95} of both action potentials.

stopped for 700 ms after the TOP corresponding to an action potential having the longer duration. Pacing was subsequently resumed at the same BCL, and, after at least another 50 stimuli had been delivered, pacing once again was stopped, this time after the TOP corresponding to an action potential with the shorter duration.

The relationship between APD and DI during constant pacing was determined by plotting APD_{95} as a function of DI. Although the resulting restitution relation was represented by a monotone increasing function without a local minimum, the time course of restitution was fit with the use of a sigmoid function to facilitate comparisons with the standard restitution relation. The r^2 coefficients for the fits with the sigmoid function were >0.98.

Isolated, perfused left ventricle. Hearts (n = 4) were excised from anesthetized adult dogs, as described above. The circumflex coronary artery was cannulated using polyethylene tubing. To avoid cutting the coronary vessels and creating vents for the perfusate, Tyrode solution was infused into the coronary artery and the approximate area of perfusion was identified by blanching of the epicardial surface. A transmural section of tissue 2–3 mm larger than the perfused area was then excised. The preparation was placed in a Plexiglas tissue chamber, where it was perfused via the coronary artery and superfused via a separate inflow with oxygenated normal Tyrode solution. A constant perfusion pressure of 50–60 mmHg (monitored using a WPI pressure transducer and BP-1 pressure transducer amplifier) was maintained by adjusting the rate of the peristaltic perfusion pump (Harvard Apparatus). The temperature was constant for any given experiment at 37–38°C.

The preparations initially were paced at a cycle length of 800 ms using a bipolar stimulating electrode. Ventricular fibrillation (VF) was induced by shortening the pacing cycle length to 100–140 ms. After 5–10 min of VF had elapsed, transmembrane action potentials were recorded from endocardial muscle using floating microelectrodes, as described above. VF was stable in these preparations for at least 60 min.

The spontaneous cycle lengths during VF were measured from the action potential recordings as the time difference between TOPs. Because of the rapid activation rates present during VF, complete repolarization occurred rarely. Consequently, measurement of APD_{95} was not possible for most action potentials. To circumvent this problem, APD was measured at a constant voltage of −70 mV. In each experiment, 100–150 measurements of cycle length and APD were obtained.

Simulated VF. For these studies, the cycle lengths that occurred during VF were measured and stored in a file. A randomly selected sequence of 50 consecutive VF cycle lengths was then delivered repeatedly to preparations of normal canine endocardium (n = 4). The entire sequence of 50 stimuli was delivered to the preparation twice without interruption to equilibrate the preparation to the rapid stimulation. During delivery of the third iteration of the sequence, pacing was interrupted for 300 ms after the 50th stimulus. The pause allowed for complete repolarization of the last action potential and a direct measurement of APD_{95}. After the pause, pacing was reinitiated, beginning with the 50th coupling interval. The entire sequence (coupling intervals: 50, 1, ..., 49) was once again delivered, and pacing was interrupted after the 49th coupling interval. Progressive rotation of the coupling intervals was continued until APD_{95} of at least 30 action potentials was measured in the absence of membrane depolarization or dislodgement of the impalement. To ensure adequate capture at these very short cycle lengths, the stimulus intensity was increased to five times the diastolic threshold and the effective refractory period of the muscle fiber was shortened by increasing the temperature of the superfusate to 39–40°C.

Data acquisition and analysis. Data acquisition was performed using a PowerComputing PowerCenter computer running at 250 MHz. Analog data were sampled at 5,000 Hz with 12-bit resolution and digitized using a National Instruments PCI-1200 DAQ board. Off-line and on-line data analysis was performed using analysis programs written in MATLAB 4.2c (The MathWorks). Curve fitting for the restitution relations was performed using TableCurve 3.1 (Jandel Scientific). The fit was optimized by adjusting the parameters of the sigmoid function to find the highest degree of freedom-adjusted r^2 coefficient. The maximal slope of the fitted function was then determined within the range of experimentally observed DI values. Results are presented as means ± SD. A two-tailed t-test for paired data was used to compare the maximal slopes of the standard and dynamic restitution curves obtained from the same fiber. One-way ANOVA was used to test for differences between muscle and Purkinje fibers and to compare the maximal restitution slopes between VF and simulated VF. A P value <0.05 was considered significant.

RESULTS

Dynamic versus standard restitution. Figure 2*A* shows a representative example of the results obtained in a ventricular muscle fiber using the dynamic restitution protocol. As the BCL was shortened progressively, a transition from a 1:1 stimulus-to-response ratio to an alternans of APD (2:2 stimulus-to-response ratio) occurred, beginning at a BCL of 195 ms. Further shortening of the BCL increased the magnitude of alternans from 9 (at BCL = 195 ms) to 27 ms (at BCL = 123 ms). At a BCL of <123 ms, 2:1 block occurred. In Fig. 2*B* APD is plotted as a function of the preceding DI. The resulting relationship is unidimensional and is approximately linear over the range of DI within which APD alternans occurred.

With the use of the dynamic restitution protocol, persistent APD alternans was obtained in all Purkinje and muscle fibers studied. The first persistent APD alternans, defined as an alternation in APD ≥5 ms persisting for >5 s, occurred at a BCL of 213 ± 22 ms in muscle and 206 ± 22 ms in Purkinje fibers [P = not significant (NS)].

A representative example of a restitution relation obtained in endocardial muscle using the standard protocol is shown in Fig. 3*A*. Also shown is the dynamic relation obtained in the same preparation. At long DI, the standard and dynamic curves were nearly parallel, whereas, at DI less than ~45 ms, the slope of the dynamic restitution curve increased, reaching a maximal slope of 1.19. In contrast, the slope of the standard curve never exceeded 0.61. Figure 3*B* shows a representative example of the standard and dynamic restitution relations obtained from a Purkinje fiber. As in endocardial muscle, the slope of the dynamic restitution relation was steeper than the slope of the standard restitution relation.

Overall, the dynamic protocol yielded a mean (±SD) maximal slope of 1.13 ± 0.13 in endocardial muscle (n = 9) and 1.14 ± 0.17 in Purkinje fibers (n = 9),

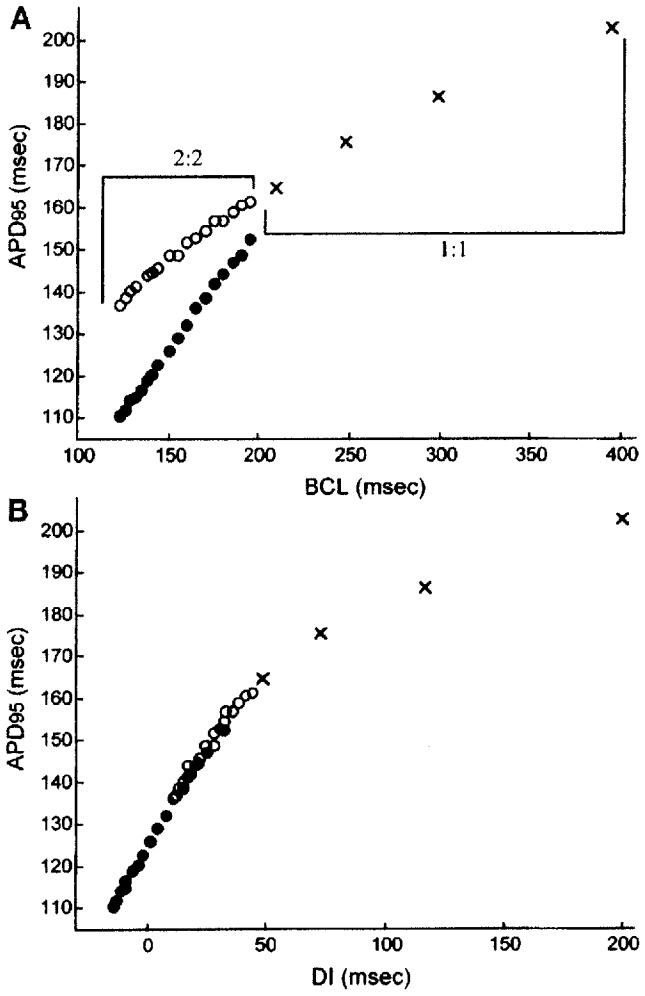

Fig. 2. *A*: sequence of action potential durations (APD_{95}) during dynamic restitution in canine endocardial muscle. During progressive shortening of basic cycle length (BCL), a transition from 1:1 stimulus-response locking (×) to 2:2 locking with alternation between long (○) and short (●) action potentials occurred. *B*: relationship between APD_{95} and preceding diastolic interval (DI) for results shown in *A*.

whereas the maximal slopes determined using the standard protocol were 0.57 ± 0.18 and 0.84 ± 0.20, respectively. The difference in slope between the dynamic and standard curves was statistically significant for both fiber types ($P < 0.001$). The difference in the slope of the standard restitution curve between Purkinje and muscle fibers also was significant ($P < 0.01$).

Iteration of restitution function. The restitution function can be iterated (14, 21) using the equations

$$APD_{n+1} = f(DI_n) \quad (1)$$

and

$$BCI_n = DI_n + APD_n \quad (2)$$

This method allows for a cobweb construct for visual iteration of the system, which is shown in Fig. 4. In Fig. 4, the restitution function f representing *Eq. 1* was determined experimentally using the dynamic protocol, and the −45° lines correspond to the BCL lines representing *Eq. 2*. Iteration of *Eqs. 1* and *2* was performed graphically by approaching the restitution function f vertically, with subsequent reflection through the BCL line. The intersection between the restitution function and the BCL line represents the fixed point of the system, and the slope of the restitution function at this point determines the dynamics of APD changes at a given BCL. If the slope is <1 (e.g., at a BCL of 300 ms), the fixed point is stable and a 1:1 stimulus-response locking results, which was also seen experimentally at this BCL (see Fig. 4*B*). APD alternans occurs when the slope at the intersection exceeds 1 and the fixed point of

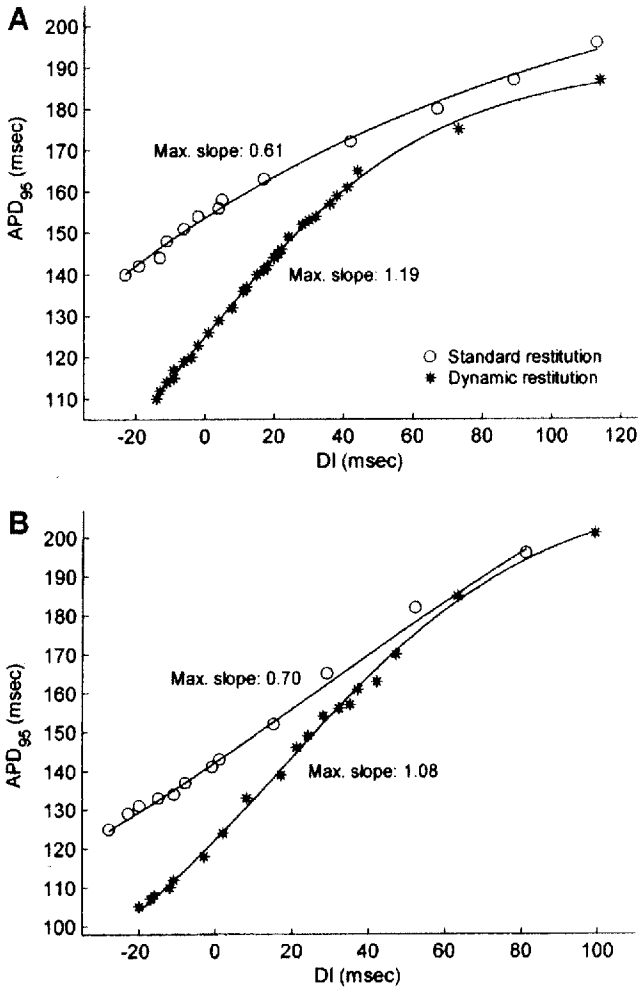

Fig. 3. *A*: representative example of standard and dynamic restitution curves obtained from the same endocardial muscle fiber as in Fig. 2. Experimental data were fit with sigmoid functions (solid lines) as described in text. Parameters of the fitted function were a = 84.0 (−1,051.2), b = 106.7 (1,273.8), c = 13.0 (−351.7), and d = 22.3 (122.9) for the dynamic (standard) curve. r^2 coefficients were 0.99 for both fits. *B*: representative example of standard and dynamic restitution curves obtained from a Purkinje fiber. Parameters of the fitted function were a = 68.2 (85.4), b = 144.6 (168.6), c = 17.1 (40.4), and d = 33.3 (59.6) for the dynamic (standard) curve. r^2 coefficients were 0.99 for both fits.

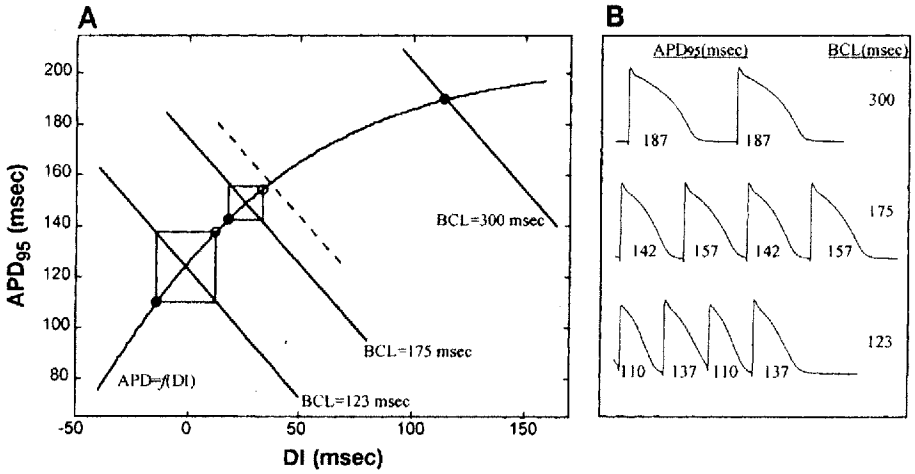

Fig. 4. *A*: iteration of the dynamic restitution function APD = *f*(DI) using the same fiber as in Fig. 2. The slope of the restitution function is <1 to the right of the dashed line and >1 to the left of the dashed line. Solid −45° lines correspond to BCL of 300, 175, and 123 ms, respectively, where BCL = APD + DI. *B*: action potential recordings corresponding to data shown in *A* for BCL = 300, 175, and 123 ms. Numbers below action potentials indicate APD_{95} in ms. See text for discussion.

the dynamical system becomes unstable. Alternans at a BCL of 175 ms is of smaller amplitude than at a BCL of 123 ms (compare with APD dynamics found experimentally at these BCL in Fig. 4*B*). Because the slope of the standard restitution relation was <1 in all of the muscle fibers and in 7 of 9 Purkinje fibers, only 1:1 locking was obtained by iterating the standard restitution relation.

Restitution during VF. Examples of action potentials recorded during VF are given in Fig. 5. The mean (±SD) cycle length during VF in four isolated, perfused canine left ventricles was 69 ± 26 ms (range 15–143 ms). An example of the relationship between APD, as measured at a constant voltage (−70 mV), and the preceding DI during VF are presented in Fig. 6*A*. Curve fitting was performed over a range of DI from 0 to 40 ms using the same sigmoid function described in *Standard restitution protocol*. The r^2 coefficients were between 0.6 and 0.8. The maximal slope of the restitution function

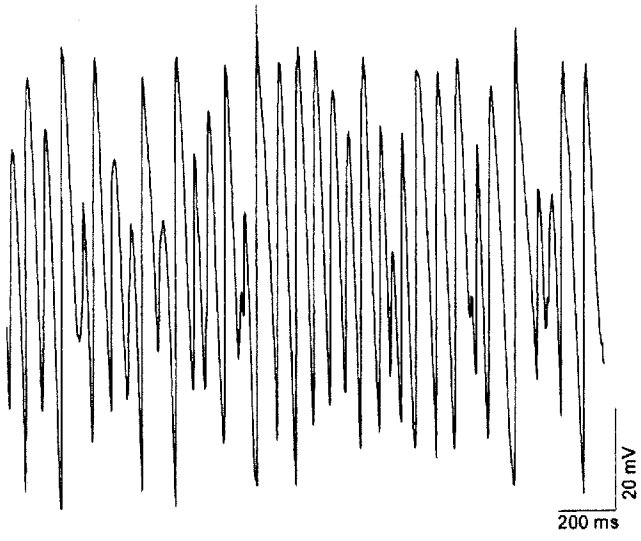

Fig. 5. Transmembrane action potential recording during an episode of ventricular fibrillation (VF) in an isolated, perfused canine left ventricle.

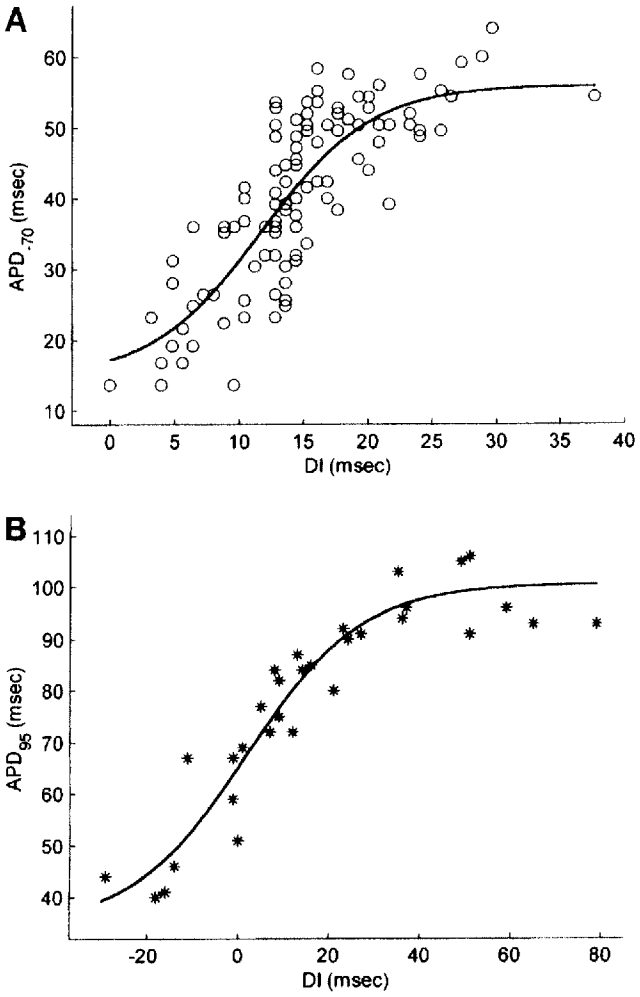

Fig. 6. *A*: restitution relationship during an episode of VF in an isolated, perfused canine left ventricle. Action potential duration was measured at a constant voltage of −70 mV (APD_{-70}) and is plotted as a function of preceding DI. Maximal slope of the fitted sigmoidal function is 2.27. *B*: relationship between APD_{95} and preceding DI during simulated VF in an endocardial muscle fiber. Maximal slope of the fitted curve is 1.32.

during VF was >1 in each episode, with a mean ± SD of 1.72 ± 0.47.

Similar results were obtained by delivering the VF cycle lengths that occurred in the isolated left ventricles to normal, superfused endocardium (simulated VF). The slope of the restitution relation obtained from this protocol also was >1 in each of the fibers studied (n = 4), with a mean ± SD of 1.44 ± 0.49 (P = NS compared with actual VF). The r^2 coefficients of the fitted sigmoid function were between 0.8 and 0.9. Figure 6*B* shows an example of the relationship between APD_{95} and DI during simulated VF.

DISCUSSION

New findings. The initial objective of this study was to reconcile two apparently conflicting experimental observations: the slope of the APD restitution relation typically has been reported to be <1, yet rapid pacing induces APD alternans, which requires that the slope of the restitution relation be equal to 1. Our approach was to measure APD restitution during APD alternans using a new automated method and to compare the resulting dynamic restitution relation with the restitution relation obtained using a standard S1-S2 protocol. The results of these studies indicated that the slope of the restitution relation during APD alternans did, in fact, equal 1, even though the slope of the standard restitution relation was <1. Our second objective was to determine whether APD dynamics during actual or simulated VF were more faithfully represented by the standard restitution relation or by the dynamic restitution relation. The results of these studies indicated that the slope of the restitution relation during actual or simulated VF exceeded 1. Accordingly, APD dynamics during VF could be accounted for, at least to a first approximation, by the dynamic restitution relation but not by the standard restitution relation.

Dynamic versus standard restitution. In this study, the slope of the standard restitution relation was found to be less steep than the slope of the dynamic restitution relation. This result was somewhat unexpected in that previous studies have shown that at short coupling intervals the slope of the standard restitution relation is steeper than that of the steady-state relation (2, 3, 9, 10). The latter is determined by measuring APD during constant pacing, as we did for the dynamic protocol. However, most studies have not paced at sufficiently short cycle lengths to induce persistent APD alternans. Consequently, the steady-state relationship between APD and DI during alternans has not been assessed. Our findings indicate that the slope of the steady-state restitution relation steepens at very short cycle lengths in association with the development of APD alternans. In fact, as discussed below, the increased slope of the restitution relation is a prerequisite for alternans. Further studies now are needed to determine whether the relationship between APD and DI that we have identified in isolated preparations pertains to the intact heart, whose behavior is influenced by loading and by the autonomic nervous system (14).

Effects of memory on restitution process. During rapid pacing, APD alternans occurred in all of the preparations studied. This result indicates that the functional relationship between APD and DI during rapid pacing must have had a slope equal to 1 (6, 13, 14, 21, 30). Although this relationship was faithfully represented by the dynamic restitution relation, only rarely did the standard restitution relation have a slope >1. The discrepancy between the results obtained using the dynamic and the standard restitution protocols may relate to differing contributions of cardiac "memory." Because the basic cycle length is constant in the standard protocol, the influence of past pacing history (memory) on the restitution of APD also is constant. In this context, the memory effect represents a slowly accumulating and dissipating (time course of seconds to minutes) influence of pacing cycle length on APD. The effects of this type of memory are evident in a downward displacement of the standard restitution relation as the pacing cycle length (S1-S1) is shortened (3, 4, 11, 19). However, the slope of the relation is reduced as the pacing cycle length is shortened (4, 10–12). Consequently, the effects of rapid pacing alone cannot account for the steeper slope of the dynamic restitution relation compared with the standard relation. Instead, the results of our previous studies suggest that beat-to-beat accumulation and dissipation of short-term memory account for the steep relationship between DI and APD during rapid pacing (13).

Dynamic restitution and electrical alternans. Iteration of the dynamic restitution curve accounts for the occurrence of both persistent and transient APD alternans. In the case of transient alternans, which is found after abrupt shortening of the BCL (25, 26), a region of the restitution function with a slope <1 is reached at the new cycle length. The dynamic system therefore gradually converges toward a stable, fixed point, which lies at the intersection of the restitution function with the new BCL line. The number of iterations before the fixed point is reached, i.e., the duration of transient alternans, again depends on the slope of the restitution curve at this intersection and is greater if the slope is closer to 1. If the fixed point is hit exactly after the change to the shorter BCL, the new steady-state APD is reached immediately and transient alternans is prevented (25).

Persistent APD alternans occurs when the slope of the restitution function at the intersection with the BCL line exceeds 1. In this case, the intersection represents an unstable fixed point, and the system diverges from this point until it locks onto a stable alternation between long and short action potentials. This behavior is manifest as a period-doubling bifurcation, where 1:1 locking is replaced by 2:2 locking as the pacing cycle length is shortened. If, in addition to a steep slope, the restitution relation contains a local minimum or maximum, more complex APD dynamics, including additional period-doubling bifurcations (2:2 to 4:4, etc.) and chaos, may occur (6, 30). It is worth noting that, although the restitution relation derived from APD alternans at different BCLs can have a slope

>1, the slope of the relationship between APD and DI during stable alternans at a given BCL is always exactly 1.

Restitution during VF. The cycle lengths observed during episodes of spontaneous VF in isolated, perfused left ventricles were comparable to those reported previously in canine hearts (1, 18, 24). Our method of simulating VF by delivering these cycle lengths to normal, superfused endocardium enabled us to repeatedly determine the effects of the VF cycle lengths on the relationship between APD and DI. The restitution kinetics during simulated VF closely resembled those during real VF, showing a nonunidimensional relationship between APD and DI with a maximal slope of the fitted sigmoid function >1. The nonunidimensional restitution relation during VF, i.e., the occurrence of more than one APD at a given DI, may arise from at least three different factors. The first is that local APD may be modulated electrotonically by conduction delay or block during VF, in which conduction block distal to the recording site would shorten APD, whereas conduction delay would prolong APD. Second, because of the marked variability in cycle lengths during VF, the influence of both short-term and long-term memory on the relationship between APD and DI is likely to vary on a beat-to-beat basis. Finally, previous studies have shown that the induction of higher-order periodic and chaotic dynamics at short pacing cycle lengths may reflect a nonmonotonic, nonunidimensional mechanism (13, 22). Consequently, variable APD at a given DI during VF may indicate the presence of such phenomena.

Implications for arrhythmogenesis. As discussed in *Dynamic restitution and electrical alternans*, a slope ≥1 creates unstable fixed points in the restitution relation that provide the basis for complex APD dynamics, including APD alternans. Bifurcations of APD and irregular APD dynamics may promote temporal and spatial heterogeneity of repolarization, which in turn may facilitate the development of reentrant arrhythmias (6–8, 15, 23, 28). In addition, heterogeneity of repolarization may underlie T wave alternans, a phenomenon that has been shown to be strongly associated with the occurrence of malignant ventricular arrhythmias and sudden cardiac death (23, 28).

Our finding that the maximal slope of the restitution relation during VF was >1 supports the hypothesis that there is a relationship among steeply sloped restitution, the occurrence of complex APD dynamics, and the development of VF (6, 15, 29). In this regard, Karma (17) has demonstrated, using a computer model of spiral waves in two-dimensional sheets of cardiac tissue, that spiral breakup occurs when the cycle length of spiral rotation is shorter than the cycle length at which the tissue develops APD alternans. APD alternans of sufficiently large amplitude causes conduction block along the wave front, precipitating the breakup of a single spiral wave into multiple smaller spirals. Although we did not examine spiral wave behavior in our preparations, the observed features of the dynamic restitution function, i.e., a steep slope leading to APD alternans of increasing amplitude with progressive shortening of the pacing cycle length, are consistent with the proposed mechanism of spiral breakup in ventricular tissue.

Our observation that complex APD dynamics during rapid pacing and during VF can be derived from the dynamic, but not from the standard, restitution relation suggests that the effects of factors known to influence the development of ventricular arrhythmias should be tested on dynamic restitution. Moreover, given that APD alternans implies a steeply sloped restitution relation, induction of alternans with rapid pacing or other techniques might be used as a surrogate for direct measurements of restitution. Those interventions that reduce the slope of dynamic restitution to values <1 would be expected to abolish APD alternans. Such an effect should correlate with a decreased risk for the development of VF. These hypotheses remain to be tested.

M. L. Koller is the recipient of a Research Fellowship Grant from the Deutsche Forschungsgemeinschaft (Ko 1782/1-1). Additional support was provided by Biotronik GmbH & Co., Berlin, Germany.

Address for reprint requests: R. F. Gilmour, Jr., Dept. of Physiology, T8 012B VRT, Cornell Univ., Ithaca, NY 14853-6401.

Received 17 March 1998; accepted in final form 27 July 1998.

REFERENCES

1. **Akiyama, T.** Intracellular recording of in situ ventricular cells during ventricular fibrillation. *Am. J. Physiol.* 240 (*Heart Circ. Physiol.* 9): H465–H471, 1981.
2. **Bass, B. G.** Restitution of the action potential in cat papillary muscle. *Am. J. Physiol.* 228: 1717–1724, 1975.
3. **Boyett, M. R., and B. R. Jewell.** A study of the factors responsible for rate-dependent shortening of the action potential in mammalian muscle. *J. Physiol. (Lond.)* 285: 359–380, 1978.
4. **Boyett, M. R., and B. R. Jewell.** Analysis of the effects of change in rate and rhythm upon the electrical activity in the heart. *Prog. Biophys. Mol. Biol.* 36: 1–52, 1980.
5. **Chen, P. S., H. S. Karagueuzian, J. N. Weiss, and A. Garfinkel.** Spirals, chaos, and new mechanisms of wave propagation. *Pacing Clin. Electrophysiol.* 20: 414–421, 1997.
6. **Chialvo, D. R., R. F. Gilmour, Jr., and J. Jalife.** Low dimensional chaos in cardiac tissue. *Nature* 343: 653–657, 1990.
7. **Chialvo, D. R., D. C. Michaels, and J. Jalife.** Supernormal excitability as a mechanism of chaotic dynamics of activation in cardiac Purkinje fibers. *Circ. Res.* 66: 525–545, 1990.
8. **Colatsky, T. J., and P. M. Hogan.** Effects of external calcium, calcium channel blocking agents, and stimulation frequency on cycle length-dependent changes in canine cardiac action potential duration. *Circ. Res.* 46: 543–552, 1980.
9. **Dilly, S. G., and M. J. Lab.** Electrophysiological alternans and restitution during acute regional ischaemia in myocardium of anaesthetized pig. *J. Physiol. (Lond.)* 402: 315–333, 1988.
10. **Elharrar, V., H. Atarashi, and B. Surawicz.** Cycle length-dependent action potential duration in canine cardiac Purkinje fibers. *Am. J. Physiol.* 247 (*Heart Circ. Physiol.* 16): H936–H945, 1984.
11. **Elharrar, V., and B. Surawicz.** Cycle length effect on restitution of action potential duration in dog cardiac fibers. *Am. J. Physiol.* 244 (*Heart Circ. Physiol.* 13): H782–H792, 1983.
12. **Franz, M. R., C. D. Swerdlow, B. Liem, and J. Schaefer.** Cycle length dependence of human action potential duration in vivo. *J. Clin. Invest.* 82: 972–979, 1988.
13. **Gilmour, R. F., Jr., N. F. Otani, and M. A. Watanabe.** Memory and complex dynamics in cardiac Purkinje fibers. *Am. J. Physiol.* 272 (*Heart Circ. Physiol.* 41): H1826–H1832, 1997.
14. **Guevara, M. R., G. Ward, A. Shrier, and L. Glass.** Electrical alternans and period doubling bifurcations. *IEEE Comp. Cardiol.* 562: 167–170, 1984.

15. **Horner, S. M., D. J. Dick, C. F. Murphy, and M. J. Lab.** Cycle length dependence of the electrophysiological effects of increased load on the myocardium. *Circulation* 94: 1131–1136, 1996.
16. **Karagueuzian, H. S., S. S. Khan, K. Hong, Y. Kobayashi, T. Denton, W. J. Mandel, and G. A. Diamond.** Action potential alternans and irregular dynamics in quinidine-intoxicated ventricular muscle cells. Implications for ventricular proarrhythmia. *Circulation* 87: 1661–1672, 1993.
17. **Karma, A.** Electrical alternans and spiral wave breakup in cardiac tissue. *Chaos* 4: 461–472, 1994.
18. **Kim, Y.-H., A. Garfinkel, T. Ikeda, T.-J. Wu, C. A. Athill, J. N. Weiss, H. S. Karagueuzian, and P.-S. Chen.** Spatiotemporal complexity of ventricular fibrillation revealed by tissue mass reduction in isolated swine right ventricle: further evidence for the quasiperiodic route to chaos hypothesis. *J. Clin. Invest.* 100: 2486–2500, 1997.
19. **Kobayashi, Y., W. Peters, S. S. Khan, W. J. Mandel, and H. S. Karagueuzian.** Cellular mechanisms of differential action potential duration restitution in canine ventricular muscle cells during single versus double premature stimuli. *Circulation* 86: 955–967, 1992.
20. **Nakaya, Y., A. Varro, V. Elharrar, and B. Surawicz.** Effect of altered repolarization course induced by antiarrhythmic drugs and constant current pulses on duration of premature action potentials in canine cardiac Purkinje fibers. *J. Cardiovasc. Pharmacol.* 14: 908–918, 1989.
21. **Nolasco, J. B., and R. W. Dahlen.** A graphic method for the study of alternation in cardiac action potentials. *J. Appl. Physiol.* 25: 191–196, 1968.
22. **Otani, N. F., and R. F. Gilmour, Jr.** Memory models for the electrical properties of local cardiac systems. *J. Theor. Biol.* 187: 409–436, 1997.
23. **Rosenbaum, D. S., L. E. Jackson, J. M. Smith, H. Garan, J. N. Ruskin, and R. J. Cohen.** Electrical alternans and vulnerability to ventricular arrhythmias. *N. Engl. J. Med.* 330: 235–241, 1994.
24. **Russell, D. C., H. J. Smith, and M. F. Oliver.** Transmembrane potential changes and ventricular fibrillation during repetitive myocardial ischemia in the dog. *Br. Heart J.* 42: 88–96, 1979.
25. **Saitoh, H., J. C. Bailey, and B. Surawicz.** Alternans of action potential duration after abrupt shortening of cycle length: differences between dog Purkinje and ventricular muscle fibers. *Circ. Res.* 62: 1027–1040, 1988.
26. **Saitoh, H., J. C. Bailey, and B. Surawicz.** Action potential duration alternans in dog Purkinje and ventricular muscle fibers. Further evidence in support of two different mechanisms. *Circulation* 80: 1421–1431, 1989.
27. **Varro, A., H. Saitoh, and B. Surawicz.** Effects of antiarrhythmic drugs on premature action potential duration in canine ventricular muscle fibers. *J. Cardiovasc. Pharmacol.* 10: 407–414, 1987.
28. **Verrier, R. L., and B. D. Nearing.** Electrophysiologic basis for T wave alternans as an index of vulnerability to ventricular fibrillation. *J. Cardiovasc. Electrophysiol.* 5: 445–461, 1994.
29. **Watanabe, M., and R. F. Gilmour, Jr.** Strategy for control of complex low-dimensional dynamics in cardiac tissue. *J. Math. Biol.* 35: 73–87, 1996.
30. **Watanabe, M., N. F. Otani, and R. F. Gilmour, Jr.** Biphasic restitution of action potential duration and complex dynamics in ventricular myocardium. *Circ. Res.* 76: 915–921, 1995.
31. **Winfree, A. T.** How does ventricular tachycardia decay into ventricular fibrillation? In: *Cardiac Mapping*, edited by M. Shenasa, M. Borggrefe, and G. Breithardt. Mount Kisco, NY: Futura, 1993, p. 657–682.